

Electronic Spectrum of Tryptophan-Phenylalanine. A Correlated Ab Initio and Time-Dependent Density Functional Theory Study

Carine Clavaguéra,^{*,†} François Piuzzi,[‡] and Jean-Pierre Dognon[¶]

Laboratoire des Mécanismes Réactionnels, Département de Chimie, Ecole Polytechnique, CNRS, 91128 Palaiseau Cedex, France, Laboratoire Francis Perrin, CEA, IRAMIS, SPAM, F-91191 Gif-sur-Yvette, France, and Laboratoire Claude Fréjacques, CEA, IRAMIS, SIS2M, F-91191 Gif-sur-Yvette, France

Received: July 22, 2009; Revised Manuscript Received: November 2, 2009

The theoretical electronic spectrum of the tryptophan-phenylalanine bichromophoric dipeptide was obtained for one of the lowest-energy conformer by various high-level computational methods such as complete active space with second order perturbation theory, second-order approximate coupled-cluster theory, and time-dependent density functional theory. The results show that the first excited state is located on the tryptophan residue and called L_b state in the amino-acid. The second and third excited states correspond respectively to the L_a state of Trp and the excited state in the Phe residue. Time-dependent density functional methods appeared to be not efficient to calculate the excited states of such a peptide (except the first one) due to the inclusion of charge transfer states.

Introduction

Tryptophan (Trp) is an important intrinsic fluorescent probe since its indole chromophore is very sensitive to its microenvironment, in a particular solvent, which strongly influences either its lifetime or its emission wavelength. This is used extensively in particular to monitor denaturation or folding of tryptophanyl proteins in condensed phase. This sensitivity to the environment is mostly due to the indole excited-state structure with the presence of two close lying states named L_a and L_b, which sensitivity to the environment is very different due to their different static dipole moments.^{1,2} Indole and its substituted derivatives have in common these two close-lying excited states, labeled as L_a and L_b (in the nomenclature of Platt,³ modified to indole derivatives by Weber⁴), with transition dipole moments orthogonal to one another. The consequence is that the tryptophan spectroscopic and dynamic properties are strongly structure dependent in peptides. To determine the relative energies of L_a and L_b, and their variation with different solvents, numerous studies were undertaken on the absorption and emission properties of 3-methyl indole. It constitutes a better model for tryptophan than indole whether it is isolated or solvated by various polar and non polar solvents.⁵ Obviously, the situation in peptides is more complex since interactions either with the backbone or other residues have to be taken into account. To acquire knowledge about more complex systems, we investigated the tryptophan-phenylalanine (Trp-Phe) isolated peptide (in gas phase). The importance of the Trp-Phe dipeptide is that some of its structures may mimic either aromatic–aromatic interactions in the folding core of proteins or aromatic–aromatic interactions in ternary or quaternary structures. In the case of the *Drosophila Bicoid* protein,⁶ a possible interaction of Trp 48 with Phe 8 when the protein is folded might contribute to the quenching of tryptophan fluorescence. These properties are also important for molecular recognition. Moreover, the fluo-

rescence quenching of Trp by phenylalanine or histidine residues have been already observed in proteins.^{6,7} Among the different possible quenching processes, some of them being still controversial, it appears from recent works by Callis et al.^{8,9} that electron transfer from indole ring to the backbone amide bond is efficient in proteins when the charge transfer state is lying very close to the S1 state. So, quenching by the peptidic backbone should constitute the major quenching process in proteins. In addition, Trp-Phe dipeptide can be considered as a fragment of opioid peptides, like Tyr-Pro-Trp-Phe-NH-2 called endomorphin-1.¹⁰ In consequence, the interactions between the Trp and Phe residues should also contribute in a non-negligible way to determine the structure of the opioid peptide. The excited state of the Trp-Phe species is expected as in tryptophan or tryptophan-derivatives to be mainly governed by interactions between the two lowest lying states L_a and L_b, since some coupling is very likely to occur due to the close energetics of both electronic states. Other processes could also occur such as conical intersections^{11,12} and electron transfer.^{13,14} The intrinsic complexity of these systems requires high level ab initio calculations in order to find the energetic picture of the excited states. Motivated by this fact, much experimental and theoretical effort has been directed at understanding the nature of these excited states and their interactions with one another.

Serrano-Andres et al.¹⁵ report a theoretical study on the excited states (singlet and triplet valence and Rydberg) of the indole molecule using the CASSCF/CASPT2 method. The two low-lying $\pi \rightarrow \pi^*$ singlet excited states, labeled ¹L_b and ¹L_a states, were computed in the gas phase at 4.43 and 4.73 eV, respectively. In addition, they found a series of low-lying Rydberg states just above the ¹L_b and ¹L_a states. They pointed out that the four singlet valence excited states are the most representative of the indole absorption spectrum. They also mentioned that the exact position and nature of the two low-lying states depend on the size, the structure, the symmetry, and the presence of substituents.

Sobolewski et al.¹² computed indole CASPT2 excitation energies at 4.30 and 4.65 eV for ¹L_b and ¹L_a states, respectively. These results are similar to those of Serrano-Andres et al.¹⁵

* To whom correspondence should be addressed. E-mail: carine.clavaguera@dcmr.polytechnique.fr.

[†] Laboratoire des Mécanismes Réactionnels.

[‡] Laboratoire Francis Perrin.

[¶] Laboratoire Claude Fréjacques.

although the basis sets and the molecular geometry are slightly different. They also investigated reaction paths and potential energy profiles for detachment of the hydrogen atom of the NH group in the lowest excited singlet state of indole ($^1\text{L}_\text{b}$, $^1\text{L}_\text{a}$, $^1\text{A}''$).

Liu et al.¹⁶ calculated the CASPT2 and ZINDO vertical excitation energies to the $^1\text{L}_\text{b}$ and $^1\text{L}_\text{a}$ states for indole. They obtained 4.31 and 4.14 eV, respectively, for the $^1\text{L}_\text{b}$ state and 4.74 and 4.64 eV for the $^1\text{L}_\text{a}$ state. Grégoire et al.¹⁷ studied the photochemistry of Trp or protonated Trp with time-dependent density functional theory (TD-DFT) and CC2 methods. More recently, Pollet et al.¹⁸ studied the excited states of the tryptophan-phenylalanine dipeptide using TD-DFT with several functionals compared with some CC2 calculations. They pointed out the well-known failure of TD-DFT for charge-transfer states.

Electronic spectroscopy of Trp-Phe had been studied experimentally by Cable et al.¹⁹ from laser desorption and supersonic molecular beam methods coupling. The detailed spectrum of these system, reveal the existence of two stable conformations with a first electronic transition energy differing by only 17 cm^{-1} . The first excitation energy was evaluated at about 4.28–4.30 eV in the gas phase. But due to the complexity of the electronic spectrum, several bands still remain unresolved. Other experimental data exist for indole in the gas phase. For example, the four low-lying excited states were evaluated at 4.37 ($^1\text{L}_\text{b}$), 4.54 ($^1\text{L}_\text{a}$), 5.26, and 5.64 eV.²⁰ These data will be used as experimental references in this work.

In the present work, we use different theoretical methods, that is, CASSCF/CASPT2, CC2, and TD-DFT to describe and understand the nature of the first excited states of the Trp-Phe dipeptide. TD-DFT is very popular to explore excited states of large molecules, but it requires to check its reliability with more sophisticated computational levels. Vertical excitation energies are calculated for the low-lying excited states and the adiabatic excitation energy for the first excited state. We also characterize the nature of the excited states with the calculation and the plotting of the difference densities upon excitation.

Methods

General Overview. For the Trp-Phe dipeptide, one can expect the existence of several stable conformers with close energies. To select the most probable structures, a potential energy surface exploration was performed with the Monte Carlo method and the AMOEBA polarizable force field^{21,22} using TINKER 4.2 software.²³ The analytical form of the force field is based on the second-order exchange-perturbation theory of intermolecular forces. The electrostatic component incorporates not only a fixed partial charge, but also a dipole and a quadrupole on each atom as derived from quantum mechanical calculations. Many-body polarization effects are explicitly treated using a self-consistent dipole polarization procedure. Inclusion of higher-order electric moments and polarization improve the performance of force field for reproducing relative conformational energies.²⁴ From this conformational sampling, several families of conformers were obtained. They can be classified as extended or compact structures with respect to the relative position of the chromophores. In each family, the most stable structure was refined with a DFT/B3LYP geometry optimization using a cc-pVDZ basis set. The vibrational frequencies were calculated at the same level of theory with the GAUSSIAN03²⁵ program and compared with the experimental vibrational spectrum in the gas phase (to be published). The low-energy structures are compact structures with essentially, in a coarse sense, parallel and perpendicular phenyl and indole rings. The latest are the most stable conformers. Among them, we have chosen to investigate the

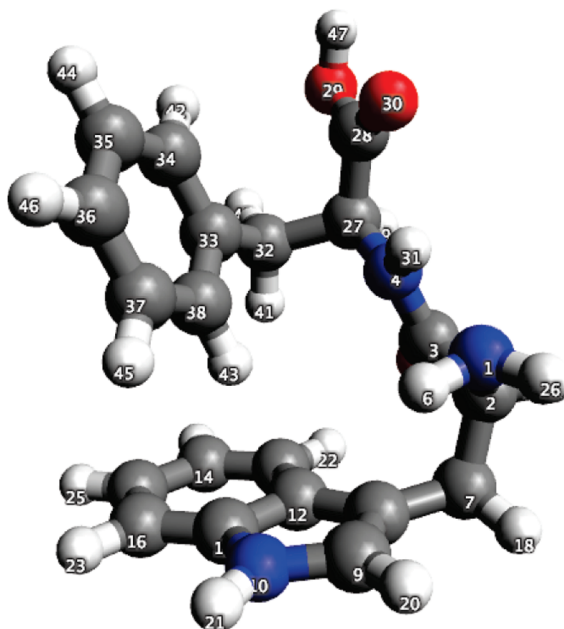


Figure 1. RI-MP2 geometry of the Trp-Phe fundamental state (nitrogen atom in blue and oxygen atom in red).

electronic spectrum of Trp-Phe from the lowest energy structure (Figure 1). This choice is reinforced by obtaining with this structure the best agreement with the experimental vibrational spectrum in the gas phase.²⁶

Excited Singlet State Energies. Vertical. To describe the nature of the excited singlet states of Trp-Phe, calculations were carried out using the CASSCF method. It was supplemented by the second-order perturbation approach CASPT2 for estimating effects of dynamic electron correlation and obtaining reference excitation energies. To describe the first four excited states, an active space including 11 electrons in 12 orbitals was defined. After the SCF convergence, the 12 molecular orbitals included in the active space were chosen on energetic criteria, by taking care that all the necessary types of molecular orbitals are present: indole, Phe residue, backbone. Owing to the large size of the calculation, we used cc-pVDZ basis set that seems to be a reasonable choice for the lower valence states. CASSCF and CASPT2 calculations were performed with the MOLCAS 6.4 software.²⁷

To study larger related systems in the future, we review the reliability of two other methods that are less computationally demanding, the CC2 coupled cluster model and the time-dependent density functional theory, the latter presently enjoying large popularity as a useful tool for extracting electronic excited state energies. The CC2 equations are an approximation to the coupled cluster singles and doubles (CCSD) ones, where the single equations are retained in the original form and the doubles equations are truncated to first order in the fluctuation potential.²⁸ We used the TURBOMOLE 5.8 program package implementation.^{29,30} The resolution-of-the-identity (RI) approximation is employed for molecular orbital two-particle integrals. The errors made within this approximation using optimized auxiliary basis sets are in general negligible as compared to errors due to the one-electron basis set incompleteness. All electrons were correlated. The RI approximation was retained for both the RI-MP2/SVP geometry optimizations and the excited-state calculations via coupled-cluster linear response theory (RI-CC2).^{31,32} All calculations have been carried out with the polarized split-valence SVP and some tests with the triple- ζ TZVPP basis sets.

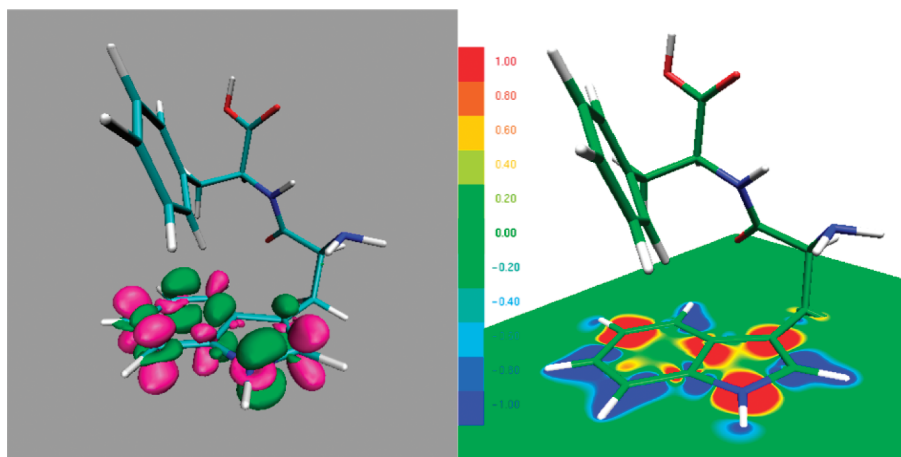


Figure 2. Plot of the difference densities at the CC2 level for the first excited state of Trp-Phe.

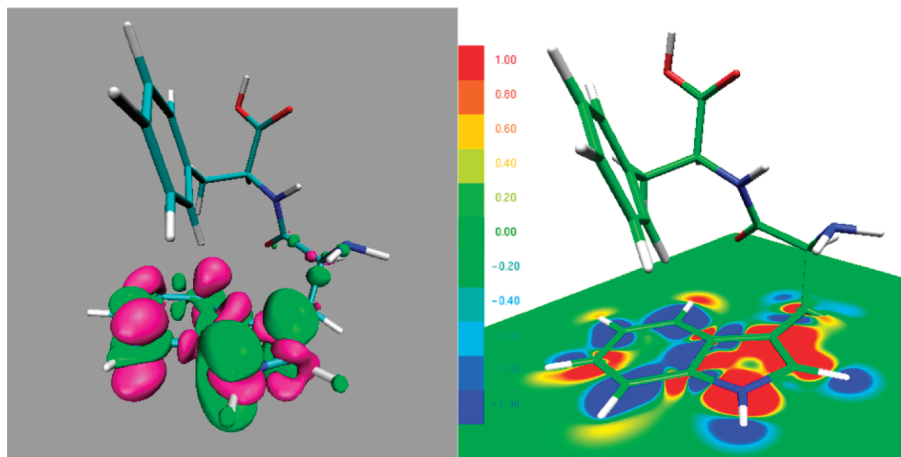


Figure 3. Plot of the difference densities at the CC2 level for the second excited state of Trp-Phe.

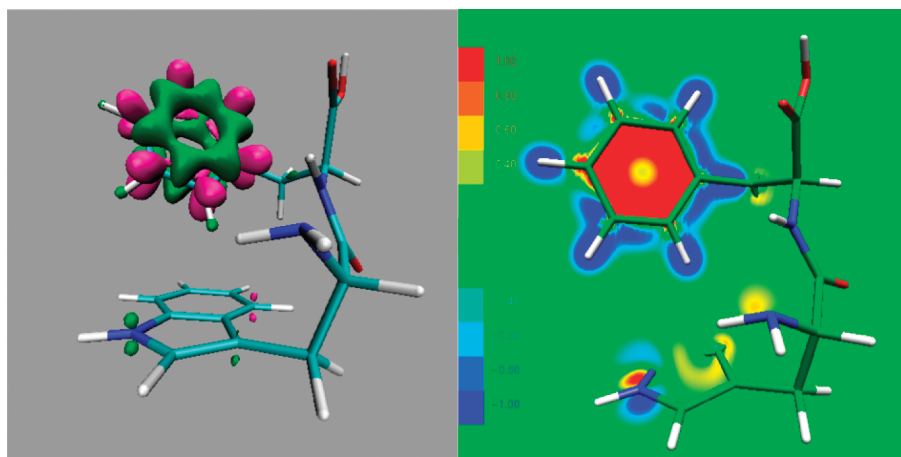


Figure 4. Plot of the difference densities at the CC2 level for the third excited state of Trp-Phe.

In addition, it is possible to characterize the nature of the excited states by plotting the difference densities produced by the excitation. The idea is to determine the changes of the density matrix upon excitations. This requires to calculate the excited-state and ground-state density matrix. For the Trp-Phe, they were obtained from RI-CC2/SVP calculations with an adapted version of TURBOMOLE 5.8 package and visualized with the VMD 1.8.6³³ and gOpenMol software.^{34,35} In Figures 2 to 5, the difference densities (volumetric and/or cut plane representation) are provided for the $S_0 \rightarrow S_n$ ($n = 1-5$) excitations (for each method, S_1 is the first excited state, S_2 is

the second, and so on). For a better legibility in the volumetric representation, the magenta and green colors stand for electron and hole, respectively, while in the cut plane representation the blue and red color stand for electron and hole, respectively.

Finally, TD-DFT calculations were performed with the B3LYP and BLYP functionals with the preceding basis sets. Geometry optimizations were performed at each DFT level, including the new implementation of dispersion corrections in the TURBOMOLE 5.10 package (B3LYP-D and BLYP-D functionals).^{29,36,37} TD-DFT calculations were also performed

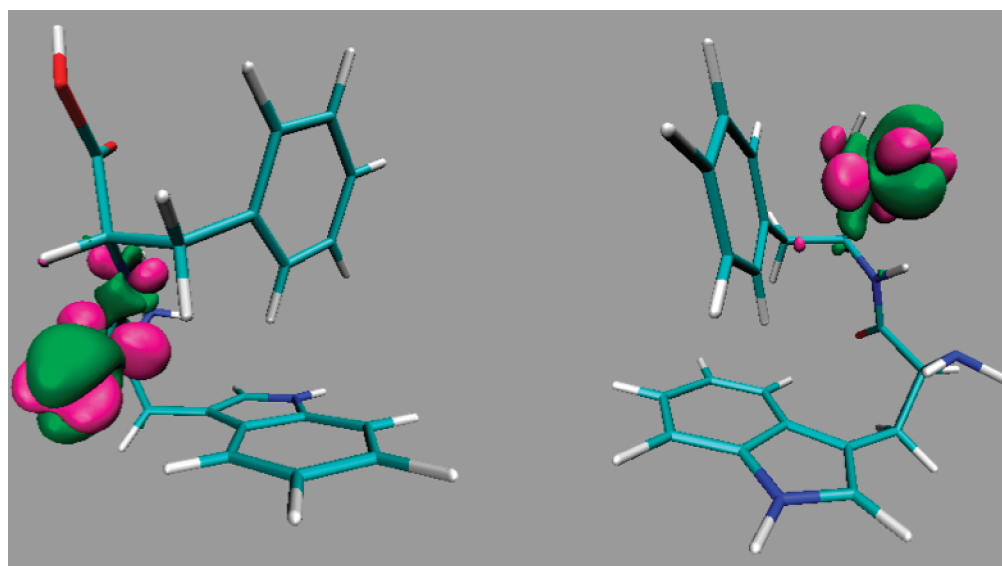


Figure 5. Plot of the difference densities at the CC2 level for the excited states number 4 and 5 of Trp-Phe.

TABLE 1: Transition Energies (eV) of the Six First Excited States in Various Methods, Oscillator Strengths in Parentheses

method	S ₁	S ₂	S ₃	S ₄	S ₅	S ₆
CASSCF	6.11	6.84	7.77	8.99		
CASPT2	4.54	4.80	5.69	5.86		
BLYP(SVP)	3.66 (0.000)	3.88 (0.001)	3.97 (0.010)	4.02 (0.000)	4.04 (0.002)	4.19 (0.001)
BLYP_D(SVP)	3.72 (0.000)	3.91 (0.010)	4.01 (0.000)	4.05 (0.000)	4.13 (0.002)	4.27 (0.006)
B3LYP(SVP)	4.69 (0.061)	4.86 (0.002)	4.92 (0.026)	4.96 (0.017)	5.27 (0.013)	5.30 (0.000)
B3LYP_D(SVP)	4.66 (0.052)	4.84 (0.007)	4.95 (0.021)	5.03 (0.003)	5.25 (0.006)	5.27 (0.002)
B3LYP(TZVPP)	4.63 (0.058)	4.80 (0.002)	4.88 (0.029)	4.91 (0.001)	5.15 (0.001)	5.27 (0.002)
B3LYP_D(TZVPP)	4.60 (0.048)	4.78 (0.007)	4.91 (0.026)	5.00 (0.002)	5.22 (0.001)	5.24 (0.003)
CC2(SVP)	4.89 (0.029)	5.16 (0.064)	5.21 (0.005)	5.77 (0.003)	6.19 (0.003)	6.36 (0.599)
CC2(TZVPP)	4.73	4.90	5.10	5.64	5.79	6.04

at the DFT-D geometries as dispersion corrections were not available for time-dependent calculations.

Adiabatic. Because of its computational cost, CASSCF or CC2 geometry optimizations could not be done on this size of system. TD-DFT with the B3LYP exchange-correlation functional was employed to perform a geometry optimization for the first excited state. As we will see it further, it is the only one that possesses the same character and a comparable transition energy as our CASPT2 reference. The purpose of this optimization is to study the existence and effects of geometrical relaxation.

Results and Discussion

Influence of the Method on the Ground-State Geometry. The RI-MP2/SVP geometry of the most stable conformer of Trp-Phe is given in Figure 1, including atomic numeration to facilitate the discussion. This RI-MP2 geometry is our reference to compare the performances of various DFT frameworks. Trp-Phe geometric parameters with various methods and basis sets are given in Table 1 in Supporting Information.

Comparing the results for SVP and TZVPP basis sets, no strong effect is observed on the geometry. The deviation for angles and dihedrals is lower than 1°. For the distances, the deviation is about 0.01 to 0.03 Å with two particular cases at 0.15 and 0.21 Å for H₂₂–O₅ (H phenyl ring) and H₁₉–O₅ (backbone) interactions respectively (B3LYP-D). The same behavior is observed in the comparison of the geometric data obtained with B3LYP and BLYP functionals. On the contrary, the geometry is strongly affected with calculations including a dispersion correction in the DFT framework, mainly in the

interaction between the two aromatic cycles. At DFT and DFT-D/BLYP levels with SVP basis sets, the deviation for angles is between 2 to 7°. Three distances are mainly affected corresponding to a stronger hydrogen phenyl ring–indole ring interaction. H₄₃–C₁₁, H₄₃–C₁₂, and H₄₃–C₁₃, with a decrease of the distances of about 0.5 Å. Furthermore, a non-negligible effect exists for the H₂₂–O₅ distance with a decrease of 0.1 Å. Similar behavior is observed at DFT and DFT-D/B3LYP levels both with SVP and TZVPP basis sets. Finally, comparing DFT-D (both BLYP and B3LYP functionals) and RI-MP2 data, the geometries are mainly similar. These geometric results show the important role of the dispersion forces in a peptide containing two aromatic residues in long-range interaction. Moreover, the B3LYP functional, widely used in the study of small peptides in gas phase, is not able to take into account the large part of these effects. It is clear that the intramolecular interactions are mainly London dispersion forces and govern the backbone-aromatic and the aromatic–aromatic interactions. This is not the case for the backbone conformational arrangement because it is dominated by hydrogen-bond interactions. Other studies have previously demonstrated such dispersion effects on the geometries of van der Waals complexes. The DFT-D framework was established to be one efficient way to take these effects into account.^{38,39}

Excited States. The CASSCF/CASPT2, TD-DFT (BLYP and B3LYP functionals), and CC2 excitation energies obtained for the six first excited states are given in Table 1. Table 2 presents a detailed analysis of the nature of the excited states for all these methods (TD-DFT BLYP and B3LYP calculations with SVP basis set are provided in Table 2 in Supporting Informa-

TABLE 2: Nature of the Six First Excited States in Various Methods

state	method	nature	MO (weight)
S1	CASPT2	$\pi \rightarrow \pi^*$	L_b indole \rightarrow indole (21% + 17%)
	B3LYP(TZVPP)	$\pi \rightarrow \pi^*$	L_a indole \rightarrow indole (88%)
	B3LYP_D(TZVPP)	$\pi \rightarrow \pi^*$	L_a indole \rightarrow indole (90%)
	CC2(SVP)	$\pi \rightarrow \pi^*$	L_b indole \rightarrow indole (63% + 13%)
	CC2(TZVPP)	$\pi \rightarrow \pi^*$	L_b indole \rightarrow indole (62% + 14%)
	CASPT2	$\pi \rightarrow \pi^*$	Phe \rightarrow Phe (20% + 16% + 16% + 15%)
S2	B3LYP(TZVPP)	CT	indole \rightarrow (Phe + CO) (89%)
	B3LYP_D(TZVPP)	CT	indole \rightarrow (Phe + CO) (89%)
	CC2(SVP)	$\pi \rightarrow \pi^*$	L_a indole \rightarrow indole (71%)
	CC2(TZVPP)	$\pi \rightarrow \pi^*$	L_a indole \rightarrow indole (67% + 13%)
	CASPT2	$\pi \rightarrow \pi^*$	L_a indole \rightarrow indole (22% + 15%)
S3	B3LYP(TZVPP)	$\pi \rightarrow \pi^* + CT$	L_b indole \rightarrow indole + indole \rightarrow (Phe + CO) (79% + 11%)
	B3LYP_D(TZVPP)	$CT + \pi \rightarrow \pi^*$	indole \rightarrow Phe + L_b indole \rightarrow indole (46% + 40%)
	CC2(SVP)	$\pi \rightarrow \pi^*$	Phe \rightarrow Phe (28% + 27% + 16% + 14%)
	CC2(TZVPP)	$\pi \rightarrow \pi^*$	Phe \rightarrow Phe (38% + 33%)
	CASPT2	$\pi \rightarrow \pi^*$	indole \rightarrow indole (22% + 18%)
S4	B3LYP(TZVPP)	CT	indole \rightarrow Phe (99%)
	B3LYP_D(TZVPP)	CT	indole \rightarrow Phe (98%)
	CC2(SVP)	$\pi \rightarrow \pi^*$	backbone(+ indole) \rightarrow (backbone + indole) (16%)
	CC2(TZVPP)	$\pi \rightarrow \pi^*$	(backbone + NH) \rightarrow CO (12%)
	B3LYP(TZVPP)	CT	indole \rightarrow (Phe + COOH) + indole \rightarrow (CO + backbone) (69% + 25%)
S5	B3LYP_D(TZVPP)	$\pi \rightarrow \pi^*$	indole \rightarrow (indole + backbone) + indole \rightarrow indole (53% + 11%)
	CC2(SVP)	$\pi \rightarrow \pi^*$	COOH \rightarrow COOH + indole(+ COOH) \rightarrow COOH (32% + 11%)
	CC2(TZVPP)	$\pi \rightarrow \pi^*$	indole \rightarrow indole (65%)
	B3LYP(TZVPP)	CT	indole \rightarrow (CO + backbone) + indole \rightarrow (Phe + COOH) (58% + 29%)
	B3LYP_D(TZVPP)	$CT + \pi \rightarrow \pi^*$	indole \rightarrow Phe + indole \rightarrow (indole + backbone) + Phe \rightarrow Phe (26% + 16% + 10%)
S6	CC2(SVP)	$\pi \rightarrow \pi^* + CT$	indole \rightarrow indole + indole \rightarrow (indole + backbone) + indole \rightarrow Phe (20% + 17% + 14%)
	CC2(TZVPP)	$\pi \rightarrow \pi^*$	COOH \rightarrow COOH (28% + 17%)

tion). CC2/SVP dipole moment of the six first excited states are provided in Supporting Information (Table 3). Complete Active Space Self Consistent Field approach is the most relevant method to study excited states of a molecule.¹⁵ Unfortunately, the Trp-Phe dipeptide is a large system for this method and the quality of the results is limited by the number of electrons and orbitals included in the calculations. However, a CASSCF calculation followed by a CASPT2 step remains the reference both for the energy and the character of the excited states.

First Excited State S₁. The transition energy of the first excited state is between 4.54 eV (CASPT2 value) and 4.76–4.89 eV (CC2 value). B3LYP and B3LYP-D calculations give similar results with both SVP and TZVPP basis sets. On the contrary, BLYP and BLYP-D results are far from the reference with an oscillator strength strictly equal to zero in comparison with 0.05–0.06 for B3LYP/B3LYP-D calculations and 0.03 for CC2 results. This low-lying $\pi \rightarrow \pi^*$ excited state can be analyzed qualitatively from the CC2 wave function (low oscillator strength, difference densities) as the 1L_b state of Trp. It is associated to the configurations related to excitations only in the indole chromophore of the tryptophan. In Figure 2, the plot of the difference densities in volumetric and cut-plane representations directly provides the loss and the gain of density located in the chromophore as a pure $\pi \rightarrow \pi^*$ state. The character of the excited state is similar whatever the method (both SVP and TZVPP basis sets) except for BLYP results. For B3LYP/B3LYP-D results, this $\pi \rightarrow \pi^*$ state corresponds to the 1L_a state of Trp, which is attributed thanks to the oscillator strength value. The energy of the 1L_a state is underestimated in DFT as previously found by Pollet et al.¹⁸

The CASPT2 energy has the best agreement with experimental excitation energy measured at 4.28–4.30 eV.¹⁹ The

calculated values are also close to the one obtained experimentally²⁰ or theoretically¹⁵ for the indole chromophore.

The vertical excitation energies give a good qualitative and semiquantitative idea of the electronic spectrum. However, in general in experimental measurements the adiabatic excitation energies are obtained and may be considerably different from the vertical estimates due to geometry relaxation. Our DFT/B3LYP results are in reasonable agreement with other methods for the first excited state, so we have performed an excited-state geometry optimization with TD-DFT followed by an adiabatic excitation energy calculation (B3LYP/SVP). The relaxation of the geometry is weak with a maximum deviation of 0.3 Å for the distances. We observe a tilt of the phenyl ring of about 8 degrees. In these conditions, for the first excited state, the TD-DFT adiabatic excitation energy is the same as the vertical excitation energy at 4.69 eV without change in the character of the state.

Higher Excited States. In CASSCF/CAPT2 framework, the second and third excited states correspond to a $\pi \rightarrow \pi^*$ excited state located in the Phe aromatic cycle and the $\pi \rightarrow \pi^*$ 1L_a excited state in the indole chromophore, respectively. The CASPT2 transition energies are 4.80 and 5.69 eV, respectively. At the CC2 level, the two states are energetically inverted with respect to the CASPT2 ones with the 1L_a and the $\pi \rightarrow \pi^*$ (phenyl ring) transition energies at 4.90 and 5.10 eV, respectively, for the TZVPP basis set and 5.16 and 5.21 eV for the SVP basis set. The difference between CASPT2 and CC2 energies can be attributed to CC2 approximations or to CAS technical limitations. The nature of the states remains the same, that is, purely $\pi \rightarrow \pi^*$ states. The difference density plots for the S₂ state in Figure 3 show a charge transfer from the pyrrole ring (which become more positive) to the benzene ring in the indole chromophore. The result is a larger permanent dipole moment for 1L_a with respect to the 1L_b one (see

Table 3 in Supporting Information). This is in good agreement with the computations of Callis on tryptophan or tryptophan derivatives.^{14,16} In Figure 4, the difference densities for the S₃ excited state confirm the $\pi \rightarrow \pi^*$ transition in the aromatic residue of Phe. Post-Hartree–Fock calculations lead to a localization of the three first excited states on the different chromophores of the dipeptide without charge transfer states, interchromophore or via the peptidic chain. The fourth excited state corresponds to another $\pi \rightarrow \pi^*$ transition on the indole chromophore associated to a transition energy of 5.86 eV in CASPT2 calculation. In the CC2 framework, S₄, S₅, and S₆ states are close in energy with 5.64, 5.79, and 6.04 eV, respectively. They correspond mainly to transitions in the backbone of the dipeptide with each state remaining localized. Some examples of this localization are given in the difference densities of states number 4 and 5 in NH₂ and COOH groups, respectively (Figure 5). No electron transfer between chromophore has been observed, so we do not have charge transfer states in CC2 calculations. Moreover, in order to check the relevance of low-lying Rydberg states for this system, we performed a CC2 calculation with an aug-cc-pVDZ basis set. The results confirm the absence of these states. An interesting feature is that the first excited state of Phenylalanine have been measured at about 4.65 eV by Martinez et al.⁴⁰ in a supersonic jet and can take place between the ¹L_b and ¹L_a states of indole. Experimental results and theoretical calculations seem to converge to say that the electronic spectrum of Trp-Phe might be built starting from the individual absorption of each fragment without coupling. The effect of the side chain is to shift the transition to higher energy.

From Table 1 and Table 2 (see also Table 2 in Supporting Information), TD-DFT results appear to be strongly different than post-Hartree–Fock ones. An important issue with using TD-DFT for large molecular systems is the introduction of spurious low-energy charge transfer states. In Table 1 and Table 2 (see also Table 2 in Supporting Information), we can observe manifestations of this phenomenon. In this case, DFT methods drastically underestimate the energies of these states with the consequence that almost all the first excited states are charge transfer states, both between the two chromophores or between one chromophore and the backbone. By comparison with CASPT2 or CC2 calculations, this charge transfer character is completely erroneous for the lowest excited states. Summarizing, as seen in Table 1, an analysis of the TD-DFT/B3LYP transition energies only gives a correct agreement with CASPT2 or CC2 results, but the nature of the excited states is completely false.

Conclusion

The main idea beyond this work is the knowledge of the excited states of Trp-Phe. Through this molecular system, we have also evaluated several theoretical methods for further calculations on large size systems. The low-lying electronic states $\pi \rightarrow \pi^*$ of Trp-Phe are essentially found from the electronic states of individual chromophore (indole and phenylalanine). From a methodological point of view, CASCF/CASPT2 is the reference method for the calculation of the excited states. But for such a large size system, it is not possible to increase the size of the active orbital space that is required to localize higher excited states as Rydberg states. The TD-DFT is proved to be no longer applicable with standard density functional. The second-order approximate coupled-cluster model CC2 with RI acceleration procedure, seems to be an accurate tool for the investigation of the excited states of large size peptides.

Acknowledgment. We would like to thank Dr. Rodolphe Pollet and Dr. Dage Sundholm for fruitful discussions. The

Center of Scientific Computing (CSC, Espoo Finland) is acknowledged for providing computer resources.

Supporting Information Available: Trp-Phe geometric parameters with various methods and basis sets (Table 1). Nature of the six first excited states from TD-DFT calculations with BLYP and B3LYP functionals and SVP basis set (Table 2). CC2/SVP dipole moment of the six first excited states (Table 3). This material is available free of charge via the Internet at <http://pubs.acs.org>.

References and Notes

- (1) Callis, P. R.; Vivian, J. T.; Slater, L. S. *Chem. Phys. Lett.* **1995**, *244*, 53–58.
- (2) Callis, P. R. *J. Chem. Phys.* **1991**, *95*, 4230–4240.
- (3) Platt, J. R. *J. Chem. Phys.* **1949**, *17*, 484–495.
- (4) Weber, G. *Biochem. J.* **1960**, *75*, 335–345.
- (5) Short, K. W.; Callis, P. R. *J. Chem. Phys.* **2000**, *113*, 5235–5244.
- (6) Subramanian, V.; Jovin, T. M.; Rivera-Pomar, R. V. *J. Biol. Chem.* **2001**, *276*, 21506–21511.
- (7) Lakowicz, J. R. *Principles of fluorescence spectroscopy*, 3rd ed.; Springer: New York, 2006.
- (8) Callis, P. R.; Vivian, J. T. *Chem. Phys. Lett.* **2003**, *369*, 409–414.
- (9) Callis, P. R.; Liu, T. *J. Phys. Chem. B* **2004**, *108*, 4248–4259.
- (10) Paterlini, M. G.; Avitabile, F.; Ostrowski, B. G.; Ferguson, D. M.; Portoghesi, P. S. *Biophys. J.* **2000**, *78*, 590–599.
- (11) Böhm, M.; Tatchen, J.; Krügler, D.; Kleinermanns, K.; Nix, M. G. D.; LeGreve, T. A.; Zwier, T. S.; Schmitt, M. *J. Phys. Chem. A* **2009**, *113*, 2456–2466.
- (12) Sobolewski, A. L.; Domcke, W. *Chem. Phys. Lett.* **1999**, *315*, 293–298.
- (13) Vivian, J. T.; Callis, P. R. *Biophys. J.* **2001**, *80*, 2093–2109.
- (14) Callis, P. R. In *Methods in Enzymology*; Brand, L., Johnson, M. L., Eds.; Academic Press: New York, 1997; Vol. 278, pp 113–150.
- (15) Serrano-Andres, L.; Roos, B. O. *J. Am. Chem. Soc.* **1996**, *118*, 185–195.
- (16) Liu, T.; Callis, P. R.; Hesp, B. H.; de Groot, M.; Buma, W. J.; Broos, J. *J. Am. Chem. Soc.* **2005**, *127*, 4104–4113.
- (17) Gregoire, G.; Jouvet, C.; Dedonder, C.; Sobolewski, A. L. *J. Am. Chem. Soc.* **2007**, *129*, 6223–6231.
- (18) Pollet, R.; Brenner, V. *Theor. Chem. Acc.* **2008**, *121*, 307–312.
- (19) Cable, J. R.; Tubergen, M. J.; Levy, D. H. *J. Am. Chem. Soc.* **1988**, *110*, 7349–7355.
- (20) Lami, H. *J. Chem. Phys.* **1977**, *67*, 3274–3281.
- (21) Grossfield, A.; Ren, P. Y.; Ponder, J. W. *J. Am. Chem. Soc.* **2003**, *125*, 15671–15682.
- (22) Ren, P. Y.; Ponder, J. W. *J. Comput. Chem.* **2002**, *23*, 1497–1506.
- (23) Ponder, J. W. *TINKER, Software Tools for Molecular Design*, Version 4.2, 2004, <http://dasher.wustl.edu/tinker/>.
- (24) Rasmussen, T. D.; Ren, P.; Ponder, J. W.; Jensen, F. *Int. J. Quantum Chem.* **2007**, *107*, 1390–1395.
- (25) Frisch, M. J. et al. *Gaussian 03*, revision C.02; Gaussian, Inc., Wallingford, CT, 2004.
- (26) Piuzzi, F., to be submitted for publication.
- (27) Karlstrom, G.; Lindh, R.; Malmqvist, P.; Roos, B. O.; Ryde, U.; Veryazov, V.; Widmark, P. O.; Cossi, M.; Schimelpfennig, B.; Neogrady, P.; Seijo, L. *Comput. Mater. Sci.* **2003**, *28*, 222–239.
- (28) Fleig, T.; Knecht, S.; Haettig, C. *J. Phys. Chem. A* **2007**, *111*, 5482–5491.
- (29) Ahlrichs, R.; Bar, M.; Haser, M.; Horn, H.; Kolmel, C. *Chem. Phys. Lett.* **1989**, *162*, 165–169.
- (30) Hattig, C.; Weigend, F. *J. Chem. Phys.* **2000**, *113*, 5154–5161.
- (31) Christiansen, O.; Koch, H.; Jorgensen, P. *Chem. Phys. Lett.* **1995**, *243*, 409–418.
- (32) Hattig, C.; Hellweg, A.; Kohn, A. *Phys. Chem. Chem. Phys.* **2006**, *8*, 1159–1169.
- (33) Humphrey, W.; Dalke, A.; Schulten, K. *J. Mol. Graphics* **1996**, *14*, 33–38.
- (34) D. L. Bergman, L. L.; Laaksonen, A. *J. Mol. Graphics Modell.* **1997**, *15*, 301–306.
- (35) Laaksonen, L. J. M. *J. Mol. Graphics* **1992**, *10*, 33–34.
- (36) Grimme, S. *J. Comput. Chem.* **2004**, *25*, 1463–1473.
- (37) Grimme, S. *J. Comput. Chem.* **2006**, *27*, 1787–1799.
- (38) Jurecka, P.; Cerny, J.; Hobza, P.; Salahub, D. R. *J. Comput. Chem.* **2007**, *28*, 555–569.
- (39) Kabelac, M.; Valdes, H.; Sherer, E. C.; Cramer, C. J.; Hobza, P. *Phys. Chem. Chem. Phys.* **2007**, *9*, 5000–5008.
- (40) Martinez, S. J.; Alfano, J. C.; Levy, D. H. *Mol. Spectrosc.* **1992**, *156*, 421–430.